

## DEVELOPING A MICRO-SCALE MODEL OF SOIL FREEZING

A. ŽÁK\*, M. BENEŠ\*, AND T.H. ILLANGASEKARE†

**Abstract.** In this contribution, we analyze thermal and mechanical effects related to the soil freezing at micro-scale. A simple 2D mechanical model of the phase transition in a pore is presented. This model is based on the Navier equations and on the continuity equation and serves mainly for a verification of the dynamics of the mechanical reaction. A basic qualitative computational study of this model is presented. Further, this model is generalized by supplementing it with a heat balance law and considering pore structure geometry onto the thermo-mechanical model describing the mutual interaction of all pore components. For this model, some basic qualitative studies, which indicate non-trivial progress of the interaction, are presented as well.

**Key words.** freezing, mathematical model, phase transition, soil, micro-scale

**AMS subject classifications.** 82B26, 74F10, 74N20

**1. Introduction.** This work is motivated by processes accompanying seasonal or climate changes affecting the upper layers of soil ground. In such cases, highly saturated soils might exhibit structural changes due to the phase transition of the wet component of soil, which introduces an uncertainty into designs of building structures in the cold regions or an ambiguity into ecological problems associated with impacts of the climate change.

The general problem of soil freezing is complex and consists of several elementary phenomena involving bulk material changes, effects due to the pore structure, and interactions of components. Although there are several macro-scale models of soil freezing phenomenon ([1], [2], [3], [4]), they are usually not sufficiently general and complex, or are one-sidedly oriented, or are based on some simplified assumptions. Most attention in the problem modeling has been devoted to the frost heave [5], the phenomenon that contributes a potential of heaving very heavy loads. The causes of this phenomenon has been also discussed using geometrical considerations at micro-scale providing its qualitative description [6]. However in contrast to the frost heave, other contributing effects has been neglected, simplified, or approximated due to their less importance or efficiency in case of the frost heaving susceptible soils.

In the regimes when the frost heave does not occur, we have a little information on how to deal with the other effects in the modeling. One of the reasons for such state of complex understanding of the freezing soil problem is that there is a few studies, experimental or theoretical, concerning with the behavior of the phenomenon at the pore-scale level. Thus one of the aims of this work is to improve the understanding of the impacts of soil freezing at such level. In particular, we provide a simple model of structural changes induced by the volumetric change of water during freezing.

**2. Artificially driven phase and structural model.** For the purpose of understanding structural dynamics of freezing water in a geometrically complex domain, we have designed a simple micro-scale mechanical model capturing both the solidifi-

---

\*Department of Mathematics, Faculty of Nuclear Sciences and Physical Engineering, Czech Technical University in Prague, Prague, Czech Republic

†Center for Experimental Study of Subsurface Environmental Processes, Colorado School of Mines, USA

cation of water in terms of local changes of its physical properties and the structural change induced by the solidification.

Although the phases at such scale are mostly distinguishable and may be located in separated subdomains, we try to study the whole medium in the pore domain via an unified description in which the phases are localized by phase indication functions.

Since this version of model has been intended to serve for the purposes of study of the model concept reliability, here we define the both phase functions artificially. Ice phase function  $\phi_i^a$  and water phase functions  $\phi_l^a$  are taken, respectively, as

$$(2.1) \quad \phi_i^a = \phi_i^a(t, \mathbf{X}) = \vartheta(t - t_0)\vartheta(\mathbf{X} - \mathbf{X}_0) \quad \text{and} \quad \phi_l^a = \phi_l^a(t, \mathbf{X}) = 1 - \phi_i^a(t, \mathbf{X}),$$

where  $\vartheta$  stands for the Heaviside step function and the functions' arguments stand for the temporal and spatial coordinates, respectively.

**2.1. Conservation laws.** Structural behavior of water-ice-grain system is given by the momentum conservation equation in the Lagrangian framework. A general form of the equation can be derived in form (similar as used in [7])

$$(2.2) \quad \mathcal{J} \varrho \frac{\partial^2 \mathbf{u}}{\partial t^2} = \nabla \cdot (\mathcal{J} \mathbf{F}^{-1} \cdot \boldsymbol{\sigma}),$$

where  $\mathcal{J}$  is the Jacobian determinant of the deformation,  $\varrho$  stands for the (current) density of material,  $\mathbf{F}$  is the deformation gradient,  $\mathbf{u}$  is the displacement vector, and  $\boldsymbol{\sigma}$  is Cauchy's stress tensor. Under the assumption of small deformations, the previous equation can be simplified, and then it reads

$$(2.3) \quad \varrho \frac{\partial^2 \mathbf{u}}{\partial t^2} = \nabla \cdot \boldsymbol{\sigma}.$$

Knowing mechanical properties of investigated materials in terms of the stress tensors, this equation can be established as the governing equation of the model for structural behavior of considered medium and its phases.

However in order to characterize phases from the mechanical point of view, first we need to specify their mechanical models, that is to define constitutional relations for deformations. Ice phase is considered to act like a homogeneous isotropic elastic material, therefore the ice stress tensor  $\boldsymbol{\sigma}_i$  might be characterized by

$$(2.4) \quad \boldsymbol{\sigma}_i = \frac{E_i}{(1 + \nu_i)} \mathbf{D}(\mathbf{u}) + \frac{\nu_i E_i \nabla \cdot \mathbf{u}}{(1 + \nu_i)(1 - 2\nu_i)} \mathbf{I},$$

where  $\mathbf{D}$  denotes the small strain tensor<sup>1</sup>,  $\mathbf{I}$  represents the unit tensor,  $E_i$  is Young's modulus of ice, and  $\nu_i$  is Poisson's ratio of ice. Liquid water phase is considered as the Newtonian fluid, so the stress tensor of the liquid phase reads

$$(2.5) \quad \boldsymbol{\sigma}_l = -p\mathbf{I} + 2\mu\mathbf{D}(\dot{\mathbf{u}}),$$

where  $p$  is the (gauge) pressure and  $\mu$  is the (dynamic) viscosity. Since the pressure represents an another independent variable in this moment, we supplement an additional relation for the liquid phase to relate the pressure and displacement. Assuming further that water is slightly compressible, we use relation

$$(2.6) \quad \frac{p}{\varrho_l E_l} + \nabla \cdot \mathbf{u} = 0,$$

---

<sup>1</sup> $\mathbf{D}(\mathbf{u}) = \frac{1}{2} (\nabla \mathbf{u} + (\nabla \mathbf{u})^T)$

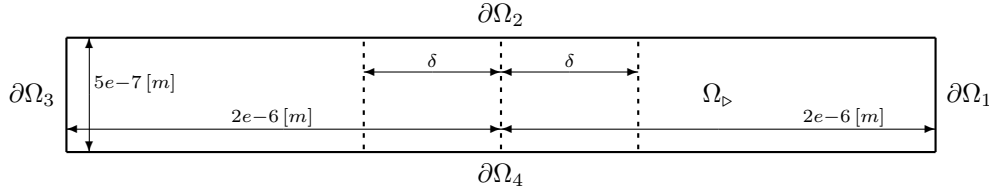


Fig. 2.1: The geometry of the considered pore volume in the initial configuration.

which can be derived from the continuity equation and is employed, e.g., in [7].

To provide the unified local expressions of terms in (2.3), we have to allow for changes in both mechanical description of the phases and mechanical state during phase transition itself. The first effect is incorporated into the model by means of the phase functions as combinations of values for single phases. From empirical knowledge, the second effect is characterized by a jump of the inner tension within the solidifying material, and we employ this by adding term  $-\phi_i^a \xi \mathbf{I}$  to the unified expression of the stress tensor. Thus the final forms of the terms read

$$(2.7) \quad \boldsymbol{\sigma} = \phi_l^a \boldsymbol{\sigma}_l + \phi_i^a (\boldsymbol{\sigma}_i - \xi \mathbf{I})$$

and

$$(2.8) \quad \varrho = \phi_l^a \varrho_l + \phi_i^a \varrho_i,$$

where  $\varrho_l$  and  $\varrho_i$  are the density of liquid water and ice, respectively.

Let the considered medium occupy pore domain  $\Omega_\triangleright \subset \mathbb{R}^2$ . Then we describe it by the system of equations in weak sense for unknowns  $\mathbf{u} = (u_1, u_2)$  and  $p$  as follows

$$(2.9) \quad (\phi_l^a \varrho_l + \phi_i^a \varrho_i) \frac{\partial^2 \mathbf{u}}{\partial t^2} - \nabla \cdot (\phi_l^a \boldsymbol{\sigma}_l + \phi_i^a [\boldsymbol{\sigma}_i - \xi \mathbf{I}]) = 0 \quad \text{in } \Omega_\triangleright,$$

$$(2.10) \quad \phi_l^a \left( \frac{p}{\varrho_l E_l} + \nabla \cdot \mathbf{u} \right) = 0 \quad \text{in } \Omega_\triangleright.$$

The system is further supplemented with boundary and initial conditions. Their particular form is discussed in the following subsection.

**2.2. Computational results.** Since the previous model incorporates discontinuous phase functions, we have simplified it for the purpose of performing simulations in order to decrease convergence difficulties. We have substituted the step function used in definitions of the phase functions for its regularized form  $\vartheta_\delta$  that provides a smooth course of transition between the original function's values on interval  $(-\delta, \delta)$ .

To demonstrate the suitability of the presented approach in the modeling of structural behavior induced by the phase transition, we have performed a parametric study in terms of the values of  $\delta$ . The study has been made for the case of the artificially solidifying water filling up a microscopic pore. The geometry of the considered pore domain is shown in Fig. 2.1, and the boundary and initial conditions are stated in Table 2.1. The study results are compared with a result of simulation of an ice expansion occurring in the same pore which is however geometrically split into two subdomains that are each occupied by a single phase and that are connected with an (non-moving) inner boundary representing the sharp mutual interface between the

Variable	Walls $\partial\Omega_1, \partial\Omega_3$	Walls $\partial\Omega_2, \partial\Omega_4$	Domain $\Omega_{\text{p}}$
$u_1$	$u_1 = 0$	$(\boldsymbol{\sigma}(\mathbf{u}) \cdot \vec{n})_1 = 0$	$u_1 _{t=0} = \dot{u}_1 _{t=0} = 0$
$u_2$	$(\boldsymbol{\sigma}(\mathbf{u}) \cdot \vec{n})_2 = 0$	$u_2 = 0$	$u_2 _{t=0} = \dot{u}_2 _{t=0} = 0$

Table 2.1: Boundary and initial conditions for geometry in Fig. 2.1. Here  $\vec{n}$  stands for the outward normal vector and  $\dot{u}$  denotes the time derivative.

phases. For the reason of drawing this comparison, we used the following definition of the phase function of ice in presented results:

$$(2.11) \quad \phi_i^a = \phi_i^a(t, \mathbf{X}) = \vartheta_{\bar{\delta}}(t - t_0 - \bar{\delta})\vartheta_{\bar{\delta}}(\mathbf{X} - \mathbf{X}_0).$$

The values of all parameters here are stated in Table 2.2 as well as the other settings of the simulations. The comparison of simulations in terms of the longitudinal displacement  $u_1$  is presented in Fig. 2.2. It shows that with decreasing  $\delta$  results approach the situation with the sharp interface between the phases. The computational results were obtained by means of the FEM package of COMSOL Multiphysics ([8]) using the quadratic Lagrange elements in space and BDF solver in time.

Symbol	Value	Symbol	Value	Symbol	Value
$\bar{\delta}$	0.02[1]	$\mu$	180[Pa · s]	$\nu_i$	0.33[1]
$\varrho_l$	1000[kg · m <sup>-3</sup> ]	$\varrho_i$	920[kg · m <sup>-3</sup> ]	$\xi$	1.3044 · 10 <sup>8</sup> [Pa]
$E_l$	5.33 · 10 <sup>9</sup> [Pa]	$E_i$	7.8 · 10 <sup>9</sup> [Pa]	$\mathbf{X}_0$	2 · 10 <sup>-6</sup> [m]

Table 2.2: Simulation settings

**3. Thermally driven phase and structural model.** In the next step of the model development, we have generalized the previous model in several aspects. Trying to involve natural conditions and principles of the freezing dynamics at this scale, we have added the thermal description of the considered domain and related the phase indication functions to the local temperature of the investigated medium. In order to increase geometry complexity, we have also included some adjacent subdomains representing rock components within porous material into our considerations. However still the smallest appropriate region of a soil pore structure has been considered.

A change of phase is naturally triggered by a change of thermo-dynamical conditions, especially of the temperature. Thus in our model, the temperature  $T$  represents the leading governing quantity for all changes within the material. When the temperature at some point passes the value of  $T_M$ , the local equilibrium between the both phases, the phase occupying the elementary volume surrounding the point changes. This leads to the obvious thermal definition of the phase functions as

$$(3.1) \quad \phi_i = \phi_i(t, \mathbf{X}) = \vartheta(T_M(\mathbf{X}) - T(t, \mathbf{X})) \quad \text{and} \quad \phi_l = \phi_l(t, \mathbf{X}) = 1 - \phi_i(t, \mathbf{X}).$$

In complex geometries at small scales, the local equilibrium is significantly influenced by the curvature of the phase interface. Assuming that the phase transition is

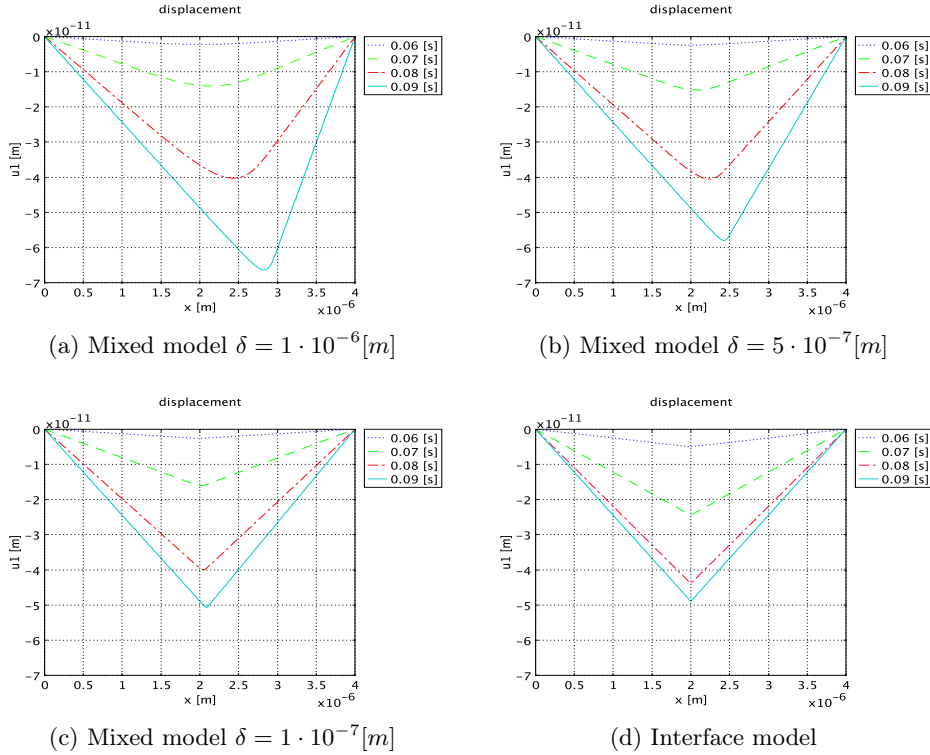


Fig. 2.2: The results of the fluid-solid structural interaction during the freezing process performed for various setting of parameter  $\delta$ . Here the interaction is caused only by the swelling effect of crystallizing ice material. The crystallization has been induced within the right-hand side half of the considered domain (Fig. 2.1) by the artificial continuous transition (2.1) starting at  $t_1 = 0.05[s]$  and culminating at  $t_2 = 0.09[s]$ . The above graphs show the **longitudinal displacement** ( $u_1$ ) along the cut of the domain running at  $x = 10^{-7}[m]$ ; the displacements are shown at times: **0.06[s]** (blue), **0.07[s]** (green), **0.08[s]** (red), **0.09[s]** (cyan).

not conducted by the pressure, the dependency between the local equilibrium temperature  $T_M$  and the local shape of interface  $\Gamma$  can be expressed by the Gibbs-Thomson equation which reads

$$(3.2) \quad \varrho_i l_M \frac{T_0 - T_M(\mathbf{X})}{T_0} = \gamma \kappa \quad \text{on } \Gamma,$$

where  $l_M$  is the specific latent heat of the phase change,  $T_0$  is the bulk freezing point,  $\gamma$  is the surface tension, and  $\kappa$  is the curvature of the phase interface.

Since we have extended our focus on all components of the saturated porous medium, the representative volume  $\Omega$  of the porous material now consists of two subdomains - one representing solid rock skeleton of the material and one representing the pore volume - and their mutual interface (see Fig. 3.1a). The interface stands for the structural boundary which can be mechanically deformed and on which we assume the continuity of both descriptive quantities and physical fluxes through the boundary.

The interface (or transition zone in case of computational simulations) between the changing phases in the pore subdomain is created thermodynamically and driven by (3.1).

Therefore the proper determination of the liquid-ice interface at any instant requires the knowledge of the distribution of  $T_M(\mathbf{X})$  within the considered pore. This can be obtained by either adding an equation for evolution of the equilibrium interface or assuming idealized symmetric geometries in which it is possible to find an analytical expression for the distribution. To keep the complexity of the model as low as possible, we make use of the latter possibility in our simulation scenarios. Then using (3.2), we simply calculate the distribution of  $T_M(\mathbf{X})$  according to the possible shapes (curvatures) of the interfaces within the particular symmetric geometry.

Considering time interval  $\mathcal{I} = (0, t_{\text{final}})$  and representative space domain  $\Omega$  with its corresponding subdivision (see Fig. 3.1a), we try to look for a solution for unknown functions  $T, \mathbf{u} : \mathcal{I} \times \Omega \rightarrow \mathbb{R}$ , where the functions are naturally (with regard to the assumptions) composed as

$$(3.3) \quad T = \begin{cases} T_s & \text{in } \Omega_s \\ T_p & \text{in } \Omega_p \end{cases}, \quad \mathbf{u} = \begin{cases} \mathbf{u}_s & \text{in } \Omega_s \\ \mathbf{u}_p & \text{in } \Omega_p \end{cases}.$$

As the heat transfer in the volume is given by the heat equation incorporating generally a term taking the phase transition of the medium in pores into consideration, the governing system of the thermo-mechanical model reads

$$(3.4) \quad \varrho c \frac{\partial T_p}{\partial t} - \varrho_i l_M \frac{\partial \phi_i}{\partial t} = \nabla \cdot (k \nabla T_p) \quad \text{in } \Omega_p,$$

$$(3.5) \quad \varrho \frac{\partial^2 \mathbf{u}_p}{\partial t^2} = \nabla \cdot \boldsymbol{\sigma} \quad \text{in } \Omega_p,$$

$$(3.6) \quad \phi_l \left( \frac{p}{\varrho_l E_l} + \nabla \cdot \mathbf{u}_p \right) = 0 \quad \text{in } \Omega_p,$$

$$(3.7) \quad \varrho_s c_s \frac{\partial T_s}{\partial t} = \nabla \cdot (k_s \nabla T_s) \quad \text{in } \Omega_s,$$

$$(3.8) \quad \varrho_s \frac{\partial^2 \mathbf{u}_s}{\partial t^2} = \nabla \cdot \boldsymbol{\sigma}_s \quad \text{in } \Omega_s,$$

$$(3.9) \quad T_s = T_p, \quad \mathbf{u}_s = \mathbf{u}_p \quad \text{on } \Gamma_{ps},$$

$$(3.10) \quad k_s \nabla T_s \cdot \mathbf{n} = k \nabla T_p \cdot \mathbf{n}, \quad \boldsymbol{\sigma}_s \cdot \mathbf{n} = \boldsymbol{\sigma} \cdot \mathbf{n} \quad \text{on } \Gamma_{ps}.$$

Here  $c$ ,  $\varrho$ ,  $k$ , and  $\boldsymbol{\sigma}$  are, respectively, the effective values of the specific heat, the density, the thermal conductivity, and the stress tensor; they are taken as

$$(3.11) \quad \varrho = \phi_l \varrho_l + \phi_i \varrho_i, \quad c = \phi_l c_l + \phi_i c_i,$$

$$(3.12) \quad k = \phi_l k_l + \phi_i k_i, \quad \boldsymbol{\sigma} = \phi_l \boldsymbol{\sigma}_l + \phi_i (\boldsymbol{\sigma}_i - \xi \mathbf{I}),$$

where subscripts  $l$  and  $i$  signify the quantities of liquid water and ice, respectively.

The system can be supplemented with boundary and initial conditions to create an initial-boundary value problem. Such particular problems are discussed in the next section.

**3.1. Computational results.** The following scenario has been designed to provide a basic information on the interaction between the freezing pore water content and the surrounding uncemented solid skeleton. The problem scenario considers a

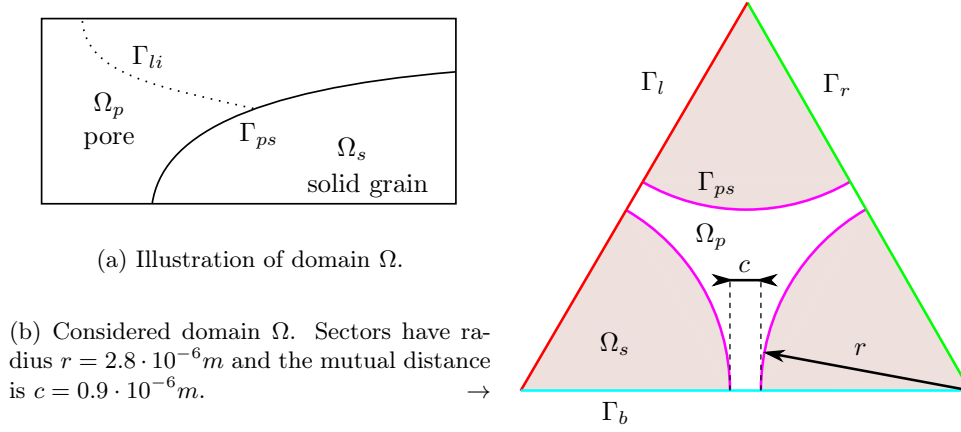


Fig. 3.1: The representative and considered domains.

Variable	Boundary $\Gamma_l$	Boundary $\Gamma_r$	Boundary $\Gamma_b$	Domain $\Omega$
$u_1$	$(\boldsymbol{\sigma}(\mathbf{u}) \cdot \vec{n})_1 = 0$	$(\boldsymbol{\sigma}(\mathbf{u}) \cdot \vec{n})_1 = 0$	$(\boldsymbol{\sigma}(\mathbf{u}) \cdot \vec{n})_1 = 0$	$u_1 _{t=0} = \dot{u}_1 _{t=0} = 0$
$u_2$	$u_2 = -\sqrt{3}u_1$	$u_2 = \sqrt{3}u_1$	$u_2 = 0$	$u_2 _{t=0} = \dot{u}_2 _{t=0} = 0$
$T$	$k\nabla T \cdot \vec{n} = q$	$k\nabla T \cdot \vec{n} = q$	$k\nabla T \cdot \vec{n} = 0$	$T _{t=0} = \dot{T} _{t=0} = 0$

Table 3.1: Boundary and initial conditions for geometry in Fig. 3.1b. Here  $\vec{n}$  stands for the outward normal vector,  $q$  is the heat flux, and  $\dot{u}, \dot{T}$  denote the time derivatives.

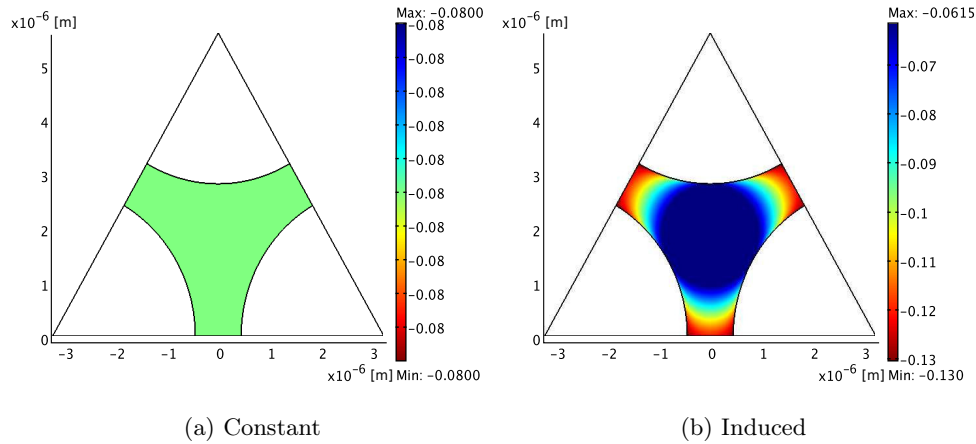
vertical cross-section through a small region of saturated soil with an ideal geometry but with the quite realistic physical dimensions and properties. The geometry comprises a group of untouched sectors, which represents the skeleton grains, and the remaining region, which stands for the pore filled with water. The particular geometry with all sizes is illustrated in Fig. 3.1b and the boundary and initial conditions are written in Table 3.1.

To stress the importance of the geometry effect, two variants of simulations have been run. One under the assumption of a constant freezing point of the water in the pore and another under the assumption of the spatially dependent freezing point distribution induced by the equilibrium condition (3.2). The maps of freezing points for the both simulations are shown in Fig. 3.2a and Fig. 3.2b, respectively. The settings of the physical parameters are stated in Table 2.2 and Table 3.2. The simulation results are shown in Fig. 3.3 and Fig. 3.4. They reveal the qualitative difference of the freezing dynamics between the two assumptions on the freezing point distribution.

**4. Conclusions.** The presented micro-scale model includes a basic heat and force balance and has been designed for the purpose of a study of structural change dynamics within saturated soils caused by the phase transition of the water content. Simulations so far provided by the model indicate non-trivial progress of the thermo-mechanical interaction, but for a general conclusion, wider testing will be needed. Results obtained from existing and future studies at this scale are planned to be used for upscaling the relevant information into our macro-scale model [9].

Symbol	Value	Symbol	Value	Symbol	Value
$\gamma$	$0.075[Pa \cdot m^{-1}]$	$\nu_s$	$0.33[1]$	$E_s$	$7.5 \cdot 10^{10}[Pa]$
$c_i$	$2.1[kJ/(kg \cdot K)]$	$c_l$	$4.2[kJ/(kg \cdot K)]$	$c_s$	$1[kJ/(kg \cdot K)]$
$k_i$	$2.18[W/(K \cdot m)]$	$k_l$	$0.6[W/(K \cdot m)]$	$k_s$	$2[W/(K \cdot m)]$
$l$	$3.34 \cdot 10^5[J \cdot K^{-1}]$	$q$	$-50[W/m]$	$T_0$	$0[^\circ C]$

Table 3.2: Simulation settings

Fig. 3.2: The freezing point distributions in  $[^\circ C]$ .

**Acknowledgments.** Partial support of the project of Czech Ministry of Education, Youth and Sports Kontakt II LH14003, 2014-2016, and of the project of the Student Grant Agency of the Czech Technical University in Prague No. SGS14/206/OHK4/3T/14 2014-2016 .

## REFERENCES

- [1] R. R. GILPIN, *A Model for the Prediction of Ice Lensing and Frost Heave in Soils*, Water Resources Research, 16/5 (1980), pp. 918–930.
- [2] A. C. FOWLER, *Secondary Frost Heave in Freezing Soils*, SIAM J. APPL. Math., 49/4 (1989), pp. 991–1008.
- [3] J. HARTIKAINEN AND M. MIKKOLA, *Thermomechanical Model of Freezing Soil by Use of the Theory of Mixtures*, in Proc. of the 6th Finnish Mechanics Days, (1997), pp. 1–6.
- [4] R. L. MICHALOWSKI, *A Constitutive Model of Saturated Soils for Frost Heave Simulations*, Cold Region Science and Technology, 22/1 (1993), pp. 47–63.
- [5] R. D. MILLER, *Frost Heaving in Non-Colloidal Soils*, in Proc. 3rd Int. Conference on Permafrost, (1978), pp. 707–713.
- [6] A. W. REMPEL, J. S. WETTLAUFER, AND M. G. WORSTER, *Interfacial premelting and the thermomolecular force: thermodynamic buoyancy*, Physical Review Letters, 87 (2001).
- [7] A. MIKELIĆ AND M.F. WHEELER, *On the interface law between a deformable porous medium containing a viscous fluid and an elastic body*, Math. Models Methods Appl. Sci., 22 (2012).
- [8] <https://www.comsol.com/>
- [9] A. ŽÁK, M. BENEŠ, AND T. H. ILLANGASEKARE, *Analysis of Model of Soil Freezing and*

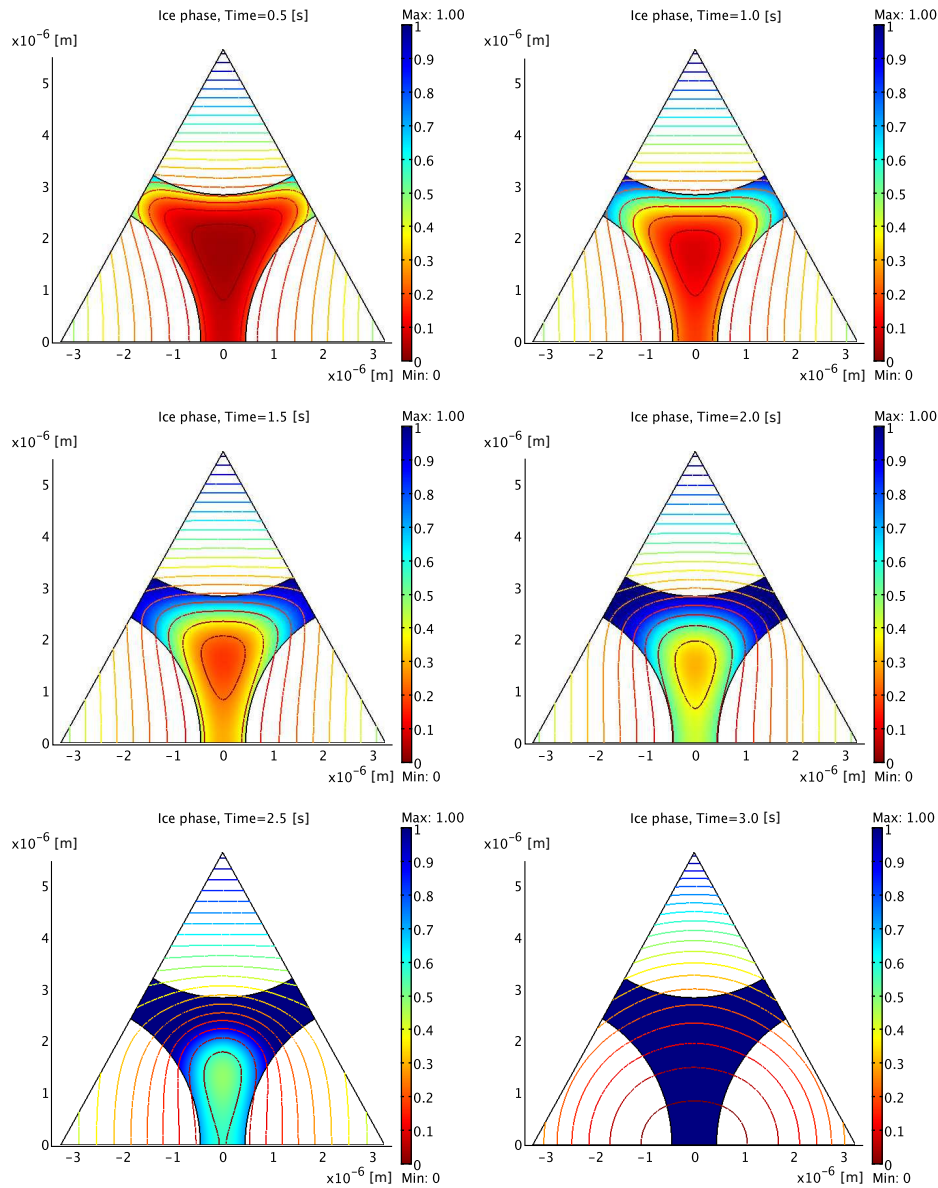


Fig. 3.3: The simulated dynamics of freezing of the considered domain. The freezing point is constant as in Fig. 3.2a. The color stands for the ice phase; the isolines signify 20 current uniformly distributed isotherms - their color legend is not shown. Here the pore water freezing depends on the temperature gradient only.

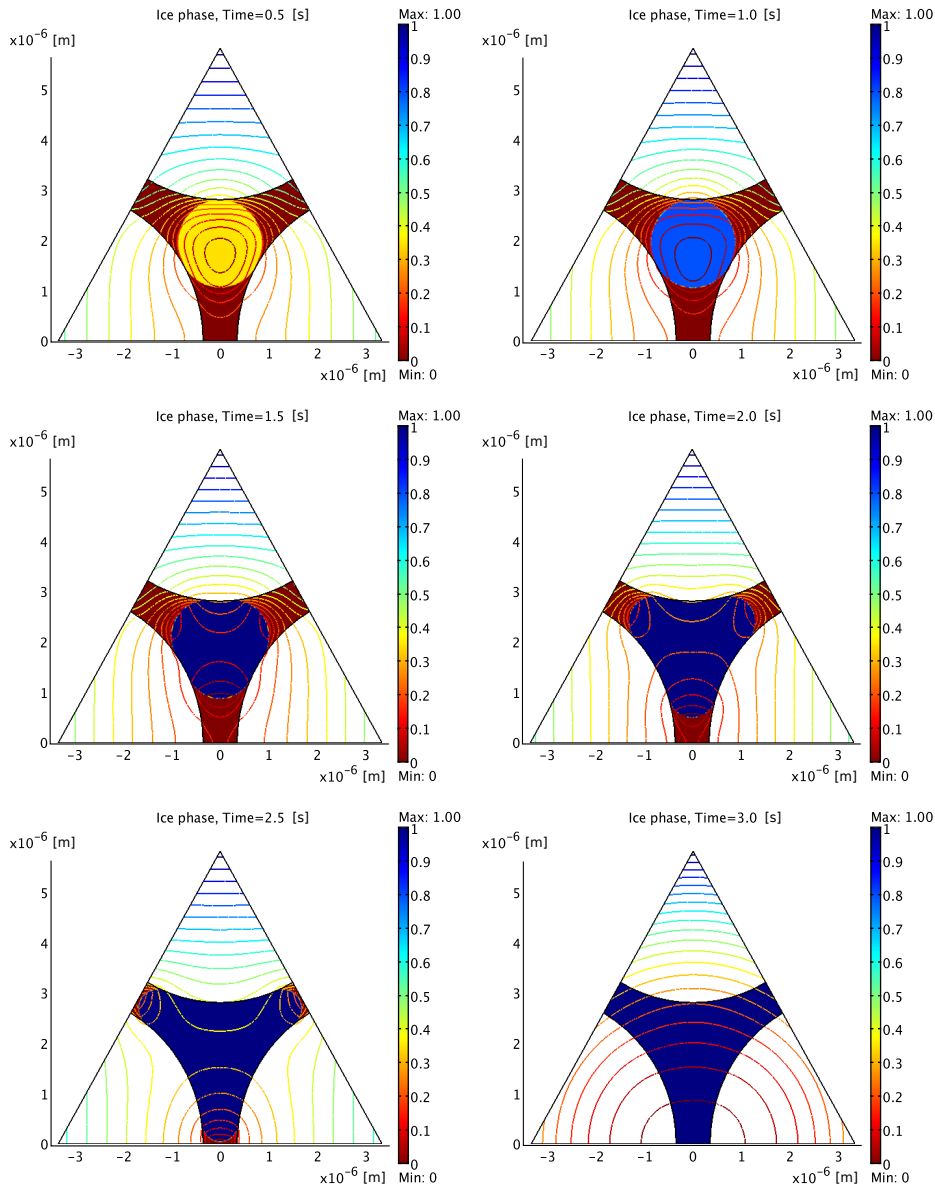


Fig. 3.4: The simulated dynamics of freezing of the considered domain. The freezing point is distributed as in Fig. 3.2b. The color stands for the ice phase; the isolines signify 20 current uniformly distributed isotherms - their color legend is not shown. If the influence of the pore geometry is encompassed, first the pore ice begins to appear within an area with the smallest curvature and then spreads further to menisci.